

Dosimetric characterization of a high dose rate ^{192}Ir source for brachytherapy application using Monte Carlo simulation and benchmarking with thermoluminescent dosimetry

N. Babaei Bidmeshki^{1*}, M. Sohrabpour¹, S.R. Mahdavi²

¹Department of Energy Engineering, Sharif University of Technology, P.O. Box 1485893169, Tehran, Iran

²Department of Medical Physics, Faculty of Medicine, Tehran University of Medical Sciences P.O. Box 1449614525, Tehran, Iran

► Technical note

ABSTRACT

Background: The purpose of this project was to derive the brachytherapy dosimetric functions described by American Association of Physicists in Medicine (AAPM) TG-43 U1 based on high dose rate ^{192}Ir sources. **Materials and Methods:** The method utilized included both simulation of the designed Polymethyl methacrylate (PMMA) phantom using the Monte Carlo of MCNP4C and benchmarking of the simulation with thermoluminescent (TL) dosimeters. **Results:** The obtained results for the radial dose function and anisotropy function showed nominal errors of less than 3% between TL measurements and the MCNP4C results. **Conclusion:** It may be concluded that due to small observed errors and the large uncertainty associated with the high dose gradients near the source point the simulation results can be used for dose estimation.

Keywords: Brachytherapy, ^{192}Ir flexisource, MCNP calculation, radiation dosimetry.

* Corresponding author:

Dr. Nadia Babaei Bidmeshki,

Fax: +98 21 44053066

E-mail:

nadia_babaei@energy.sharif.ir

Received: May 2013

Accepted: Oct. 2013

Int. J. Radiat. Res., July 2014;
12(3): 265-270

INTRODUCTION

Brachytherapy is the clinical use of small encapsulated radioactive sources at a short distance from the target volume for irradiation of malignant tumors. Permanent implant brachytherapy has long employed radionuclides that emit principally low-energy gamma rays that can be produced to provide suitable activity⁽¹⁾. Valid clinical application for treatment planning requires reliable data of the dosimetric characteristics of a new source design. Since currently varieties of ^{192}Ir sources are commercially available with different core and encapsulation dimensions, accurate dosimetry are required in the close vicinity of the HDR

iridium sources.

Both theoretical and experimental methods have been widely used to characterize two dimensional dose distributions around brachy sources in water mediums⁽²⁻⁴⁾. Monte Carlo simulation, film dosimetry and thermoluminescent dosimetry (TLD) are used for determination of dose distribution around sources in different media⁽⁵⁻⁷⁾. The aim of this work is calculating the dosimetric data of an HDR ^{192}Ir seed source (Flexisource) and also comparing the results with the obtained data from TL dosimeters within a PMMA phantom. The data is used for dose distribution measurements around the Flexisource in the after loading Flexitron system.

MATERIALS AND METHODS

Source description

The radiation source used in this investigation was a HDR ^{192}Ir , Flexisource (Veenendaal, The Netherlands), with an initial activity of 370 GBq at the time of manufacturing. The geometric design of the Flexisource is shown in figure 1. The active core of the source is a pure iridium cylinder (density 22.42 g/cm^3) with an active length of 3.5 mm and a diameter of 0.6 mm. The active core is covered by a stainless-steel-304 capsule (density 8 g/cm^3) with outer source dimensions of 0.85 mm and 4.6 mm for diameter and length, respectively. It was assumed that the radioactive material was uniformly distributed within the ^{192}Ir active core (8).

The decay scheme of ^{192}Ir was available on-line in the Nuclear Data Base of the IAEA. The gamma emission spectrum of ^{192}Ir is shown as a histogram representation in figure 2. The source is normalized to one Bq of ^{192}Ir . This is achieved by using the 'sum of the emission probabilities for all photons' per decay ($=2.363$) of ^{192}Ir (9). It was observed by Mowlavi *et al.* that the real spectrum rather than monochromatic spectra with energy of 356 keV was important for dose calculation near and far from the source (10). The β spectrum of the ^{192}Ir source has not been considered since its contribution to the dose rate distribution for distances greater than 1 mm from the source is negligible due to source encapsulation.

Phantom design

In selection of a calibration or dosimetric phantom a number of key parameters of the phantom, including thickness for production of

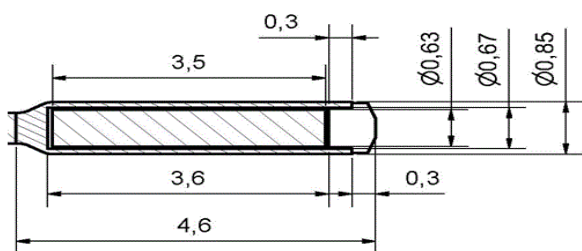


Figure 1. Schematic diagram of the ^{192}Ir Flexisource (dimensions in millimeter).

the full scattering condition and the composition of tissue substitute must be taken into account. For photons the effective atomic number of the material is important. Water, acrylics, polystyrene or similar low atomic number materials are appropriate for such phantoms (11). Polymethyl methacrylate (PMMA) is one such material with low effective atomic number ($Z_{\text{eff}}=6.5$) that is found suitable for calibration and dose measurements. In this work a PMMA slab phantom of dimensions $30 \times 30 \times 20 \text{ cm}^3$ was used to measure the dose distribution around the source. This phantom was designed with a central hole for insertion of the source carrier applicator which was perpendicular to the axis of the TLD discs. The TLD discs were arranged in circular forms with a radial distribution in the range of 0.5 to 9 cm and were placed perpendicular to the source axis. Figure 3 shows the picture of the geometric design of the phantom.

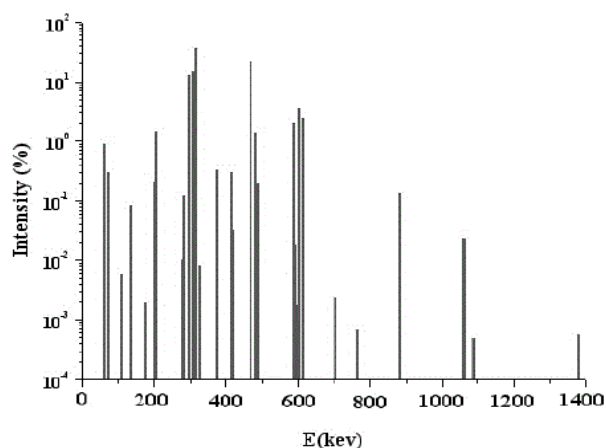


Figure 2. The real spectrum of ^{192}Ir .



Figure 3. Geometric design of the PMMA phantom.

Monte Carlo simulation

The Monte Carlo code system MCNP4c was employed for the simulation. MCNP is a general purpose Monte Carlo radiation transport code which can simulate coupled neutron-photon-electron transport in three dimensions through complex geometries constructed as Boolean combinations of planes, spheres, cones and cylinders. This code transports photon and electrons in the energy range from 1 keV to 100 MeV. The detailed photon physics treatment includes photoelectric absorption; K- and L- shell fluorescence, Auger emission, coherent scattering with electron binding effects accounted for by form factors, and incoherent scattering. A photoelectric event is considered to be absorption and the photon history is terminated in such an interaction. In the case of a Compton interaction, the final energy and position of the photon are randomly sampled from Klein-Nishina relation based angular probability and energy distribution functions (12). The code was run in combined photon electron mode. An energy cut off value of 1 keV was used to terminate tracking of photon and electron histories. MCNP requires the source for a particular problem to be specified in a user-defined input file. The source includes distributions of the positions, energy and angle of the starting particles. The MCNP tally options utilized for the needed parameters was *F8 tally with Mode p e. The cross section library containing data from the ENDF was included with the MCNP code that was utilized for the computations.

Thermoluminescent dosimeters

TLD-100H (Harshaw) discs with diameter length of 4.5 mm × 0.9 mm thickness were used in this study. The protocol for using TLD-100H was described in detail by Mckeever et al. and Furetta (13-14). Briefly, the discs were first annealed at 240°C for 10 min. To determine the sensitivity of each individual TLD, efficiency correction coefficients (ECC) were obtained by the following equation:

$$Ecc_i = \bar{R} / (R_i - R_{bkg}) \quad (1)$$

Where Ecc_i is the efficiency correction coefficient for each TLD disc, R_i and \bar{R} are individual and average readings of the total TLDs respectively. This correction factor is due to differences in TLD's physical properties such as size, mass, etc. For calibration purposes TLD discs were placed under Plexi-glass plates for electronic equilibrium and were irradiated from a calibrated Co-60 source. To obtain the absorbed dose calibration factor in Gy/Count, TLD discs in groups of five were irradiated with different doses from 0.3 Gy to 5 Gy. Then to calculate the corrected reading of each field dosimeter the followed equation was used (14):

$$D_w = (R_i - R_{bkg}) \times Ecc_i \times CF \quad (2)$$

Dosimetric formalism

The dose rate at a point (r, θ) in the phantom around the ^{192}Ir source was determined following the protocol introduced by group 43 AAPM using the following equation (15-16):

$$\dot{D}(r, \theta) = S_k \Lambda \frac{G_L(r, \theta)}{G_L(r_0, \theta_0)} g_L(r) F(r, \theta) \quad (3)$$

where r denotes the distance from the center of the active source to the point of interest, r_0 denotes the reference distance, and θ denotes the polar angle specifying the point of interest relative to the source longitudinal axis, and θ_0 is the reference angle. The definitions of the denoted parameters are shown in figure 4.

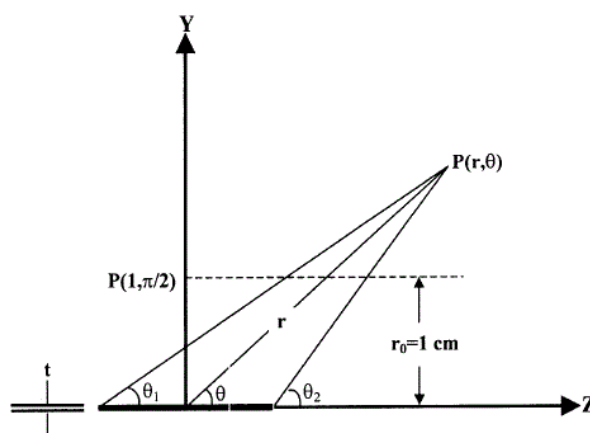


Figure 4. Coordinate system used for the dosimetry calculation formalism (Update of AAPM TG-43 report).

In equation 3, $D(r,\theta)$ is the dose rate at point (r,θ) , S_k is the source strength (air-kerma strength), Λ is dose rate constant, $G_L(r,\theta)$ is geometry factor, $g_L(r)$ is the radial dose function, and $F(r,\theta)$ is anisotropy function.

Geometry function is used to improve the accuracy with which dose rates can be estimated by interpolation from data tabulated at discrete points. Physically, the geometry function neglects scattering and attenuation, and provides an effective inverse square law correction based on an approximate model of the spatial distribution of radioactivity within the source. Because the geometry function is used only to interpolate between tabulated dose rates values at defined points, highly simplistic approximations yield sufficient accuracy for treatment planning:

$$G_L(r,\theta) = \begin{cases} \frac{\beta}{Lr \sin \theta} & \text{if } \theta \neq 0 \\ \frac{1}{r^2 - L^2/4} & \text{if } \theta = 0 \end{cases} \quad (4)$$

for line-source approximation, where β is the angle, in radians, subtended by the tips of the hypothetical line source with respect to the point of interest (r,θ) .

The radial dose function accounts for dose fall-off on the transverse plane due to photon scattering and attenuation, i.e., excluding fall-off included by the geometry function:

$$g_L(r) = \frac{\dot{D}(r,\theta_0)}{\dot{D}(r_0,\theta_0)} \cdot \frac{G_L(r_0,\theta_0)}{G_L(r,\theta_0)} \quad (5)$$

The 2-D anisotropy function describes the variation in dose distribution around the source, including the effects of absorption and scatter in the medium as a function of polar angle relative to the transverse plane due to self-filtration, oblique filtration of primary photons through the encapsulating material and scattering of photons in the medium. 2-D anisotropy function is defined as:

$$F(r,\theta) = \frac{\dot{D}(r,\theta)}{\dot{D}(r,\theta_0)} \cdot \frac{G_L(r,\theta_0)}{G_L(r,\theta)} \quad (6)$$

RESULTS AND DISCUSSION

The radial dose function, $g(r)$, was calculated according to the TG-43 definition and is depicted in table 1. Figure 5 details both simulated and measured data for the Flexisource. Comparison of the measured and simulated data is The radial dose function, $g(r)$, was calculated according to the TG-43 definition and is depicted in table 1. Figure 5 details both simulated and measured data for the Flexisource. Comparison of the measured and simulated data is found to be nominally less than 3%. For this source, the Monte Carlo calculated $g(r)$ function in the range of 0.5 to 9 cm was fitted using a fifth-order polynomial curve, namely

$$g(r) = a_0 + a_1r + a_2r^2 + a_3r^3 + a_4r^4 + a_5r^5 \quad (7)$$

where $a_0=0.7027$, $a_1=0.4847$, $a_2=-0.2513$, $a_3=0.0574$, $a_4=-0.006$, $a_5=0.0002$.

Table I. A comparison of the calculated and measured radial dose function of the Flexisource ^{192}Ir brachytherapy source.

r(cm)	g(r), simulation	g(r), measurement	Relative difference percent
0.6	0.91	0.82	10.01
1	1	1	0
2.4	1.03	1.01	2.15
3	1.02	1.02	0
3.7	0.98	0.96	3.7
4.5	0.98	0.9	7.5
5.2	1.01	1.03	1.94
7.5	0.99	0.97	2.02
9	0.84	0.81	3.6

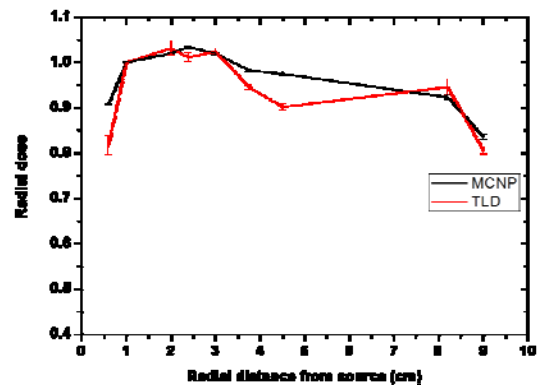


Figure 5. Comparison of the measured dose function, $g(r)$, of the Flexisource with the Monte Carlo simulated data in PMMA phantom.

The results of the two-dimensional measurements of the dose distribution in phantom were analyzed using the geometry factor, $G(r,\theta)$, to arrive at an anisotropy function for the Flexisource. Figures 6(a) and 6 (b) detail both simulated and measured data for the Flexisource. Nominal relative differences with respect to Monte Carlo simulation are found to be 10% at angles between 0 to 30 degree and less than 2% at other angles. The greater errors between simulated and measured $F(r,\theta)$ for the angles of 90 to 150 degrees is partially due to the transit dose which depicts itself as a higher value of the measured data at these angles. This same transit dose phenomenon also presents itself as an asymmetric dose distribution with higher values occurring at angles 90 to 150.

Figure 7 presents a comparison of the radial dose functions for various ^{192}Ir HDR sources. It indicates that radial dose functions

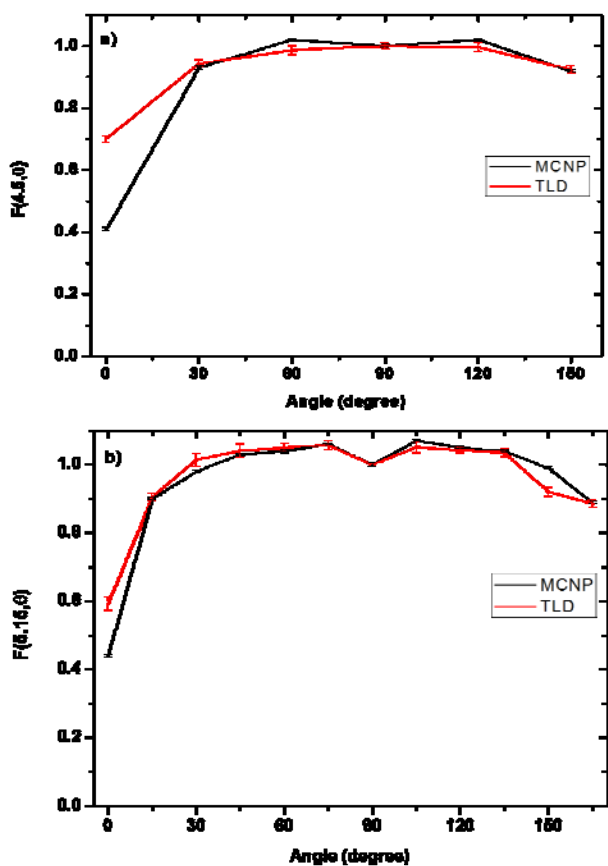


Figure 6. Comparison of the measured and Monte Carlo calculated anisotropy function for the Flexisource in a PMMA phantom at radial distances of (a) $r=4.5$ cm, and (b) $r=5.2$ cm.

are very similar for these HDR sources. The discrepancies between the radial dose functions far from the source ($r > 5$ cm) arise from the different sizes of the water phantoms (8).

In figure 8, the anisotropy functions of various ^{192}Ir HDR sources are compared for $r = 1$ cm. It shows that the anisotropy function is very similar for Flexisource, Nucletron mHDR-v2, BEBIG-HDR, and Gammamed 12i sources due to their similar geometric design. In contrast, significant differences exist between the anisotropy function of these sources and that of the Buchler source. This is due to the larger distance from the active edge to the tip of the source, the larger active diameter, and a larger filtration capsule thickness for the former source model compared with the other ones (8).

In view of the very high dose gradient near the source point, the actual measurement may have large associated uncertainties. On the other

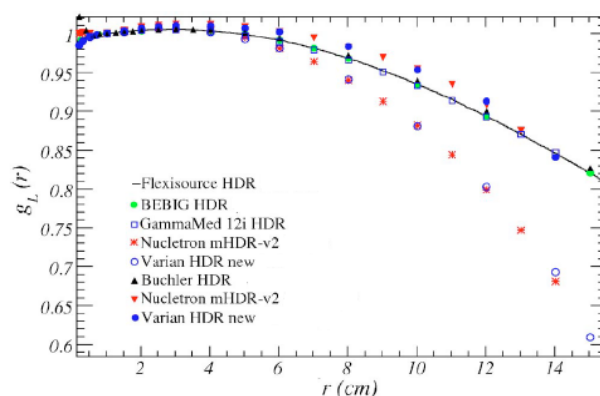


Figure 7. Comparison of the radial dose functions for various ^{192}Ir HDR sources.

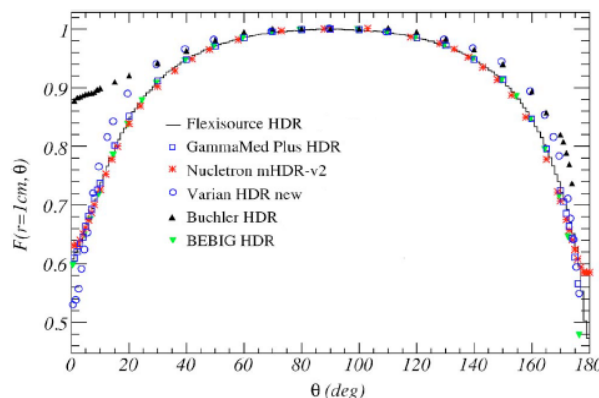


Figure 8. Comparison of the anisotropy functions for various ^{192}Ir HDR sources for the radial distance of $r = 1$ cm.

hand, simulated dose measurements at any distance near or far away from the source point can be performed with reasonable accuracy, and thus it may be feasible to partially rely on the simulated data in places where dosimetry is difficult to carry out.

CONCLUSIONS

The dosimetric characteristic of the Flexisource ^{192}Ir brachytherapy source by AAPM TG-43 formalism has been performed using standard methods employing thermoluminescent dosimeters in a water equivalent phantom. The results of this study indicate that Monte Carlo simulation in brachytherapy is useful to obtain dosimetric parameters and to verify the measurement data.

ACKNOWLEDGEMENTS

The authors would like to express their appreciation to Mr. Arjang Shahvar for his technical support in this study.

REFERENCES

1. Baltas DS, Sakelliou L, Zamboglou N (2007) The Physics of Modern Brachytherapy for Oncology. Taylor & Francis Group, New York.
2. Ghiassi-Nejad M, Jafarizadeh M, Ahmadian-Pour MR, Ghahramani AR (2001) Dosimetric characteristics of ^{192}Ir sources used in interstitial brachytherapy. *Appl Radiat Isot*, **55**: 189-195.
3. Duggan DM (2004) Improved radial dose function estimation using current version MCNP Monte-Carlo simulation: Model6711 and ISC3500 ^{125}I brachytherapy sources. *Appl Radiat Isot*, **61**: 1443-1450.
4. Wang Z and Hernel NE (2005) Determination of dosimetric characteristics of optiSeed a plastic brachytherapy ^{103}Pd source. *Appl Radiat Isot*, **63**: 311-321.
5. Sellakumar P, Sathishkumar A, Supe SS, Anand MR, Nithya K, Sajitha JF (2009) Evaluation of dosimetric functions for ^{192}Ir source using radiochromic film. *Nucl Instrum Methods*, **267**: 1862-1866.
6. Sowards KT and Meigooni AS (2002) A Monte Carlo evaluation of the dosimetric characteristics of the Best Model 2301 ^{125}I brachytherapy source. *Appl Radiat Isot*, **57**: 327-333.
7. Wallace RE (2002) Model 3500 ^{125}I brachytherapy source dosimetric characterization. *Appl Radiat Isot*, **56**: 581-587.
8. Granero D, Perez-Calatayud J, Casal E, Ballester F, Venselaar J (2006) A dosimetric study on the ^{192}Ir dose rate Flexisource. *Med Phys*, **33**: 4578-4582.
9. Borg J and Rogers DWO (1999) Spectra and air-kerma strength for encapsulated ^{192}Ir sources. *Med Phys*, **26**: 2441-2444.
10. Mowlavi AA, Cupardo F, Severgnini M (2008) Monte Carlo and experimental relative dose determination for an ^{192}Ir source in water phantom. *Iran J Radiat Res*, **6**: 37-42.
11. ICRU Report 48 (1992) Phantoms and computational models in therapy, diagnosis and protection. ICRU Publication, Bethesda.
12. Los Alamos National Laboratory (2000) MCNP4c: Monte Carlo N-particle transport code system. Oak Ridge National Laboratory, New Mexico.
13. McKeever SWS, Moscovitch M, Townsend PD (1995) Thermoluminescence Dosimetry Materials, Properties and Uses. Nuclear Technology Publishing, Ashford.
14. Furetta C (2003) Handbook of the Thermoluminescence. World Scientific Publishing, Singapore.
15. Rivard MJ, Coursey BM, Deward LA, Hanson WF, Huq MS, Mitch MG, Nath R, Williamson JF (2004) Update of AAPM Task Group No. 43 Report: a revised AAPM protocol for brachytherapy dose calculations. *Med Phys*, **31**: 633-674.
16. Yue NJ (2007) Principles and practice of brachytherapy dosimetry. *Radiat Measur*, **41**: 522-527.